Available online at www.sciencedirect.com
ScienceDirect
JOURNAL OF RARE EARTHS
www.re-journal.com/en/
JOURNAL OF RARE EARTHS, Vol. 27, No. 3, Jun. 2009, p. 425

Ceria modified three-dimensionally ordered macro-porous Pt/TiO_2 catalysts for water-gas shift reaction

LIANG Hao (梁　皓), ZHANG Yuan (张　媛), LIU Yuan (刘　源)

(Tianjin Key Laboratory of Applied Catalysis Science and Engineering, Department of Catalysis Science and Technology, School of Chemical Engineering and Technology, Tianjin University, Tianjin 300072, China)

Received 7 October 2008; revised 28 February 2009

Abstract: Three-dimensionally ordered macro-porous (3DOM) TiO_2 and ceria-modified 3DOM TiO_2 supported platinum catalysts were prepared with template and impregnation methods, and the resultant samples were characterized by scanning electron microscopy(SEM), X-ray diffractometer(XRD), high-resolution transmission electron microscopy(HRTEM) and temperature programmed reduction(TPR) techniques. The catalytic performances over the platinum-based catalysts were investigated for water-gas shift (WGS) reaction in a wide temperature range (180–360 °C). The results showed that 3DOM Pt/TiO_2 catalyst exhibited obviously better catalytic performance than the corresponding non macro-porous catalyst, owing to the macro-porous structure favoring mass transfer. Addition of ceria into 3DOM Pt/TiO_2 led to improvement of catalytic activity. TPR and HRTEM results showed that the interaction existed between ceria and titanium oxide and addition of ceria promoted the reducibility of platinum oxide and TiO_2 on the interface of platinum and TiO_2 particles, which contributed to high activity of the ceria modified catalysts. The results indicated that ceria-modified 3DOM Pt/TiO_2 was a promising candidate of fuel cell oriented WGS catalyst.

Keywords: three dimensionally ordered; ceria; macro-porous; water gas shift; platinum; rare earths

Water-gas shift (WGS) as a potential pure hydrogen production reaction has recently been attracting growing interest due to development of fuel cell power system. Conventional low-temperature ($Cu/ZnO-Al_2O_3$) and high-temperature (Fe_3O_4/Cr_2O_3) WGS catalysts can not be used in such application, due to their complex and time-consuming activation protocol before use, instability in contact with air, narrow temperature window of usage and relatively low activity[1]. Noble metal/reducible oxide systems have advantages not shown by the traditional catalysts as they can combine high activity and stability[2]. Among these systems, Pt/TiO_2 catalyst seems to be most promising, exhibiting good catalytic performance[3]. Ceria is also particularly interesting as candidate to mix with TiO_2 substrates, because ceria has special properties beneficial for WGS[4,5].

Three dimensionally ordered macro-porous (3DOM) materials are characterized with pore size in several hundreds to several tens of nano-meter, and with ball shape pores which are closely packed with a high degree of order and interconnected to each other through small windows. Owing to this special pore structure, 3DOM materials are widely studied for application in absorption and separation process, catalytic supports, photocrystals and ceramics materials[6,7].

As for using 3DOM materials as catalysts or catalyst supports, several reports can be found on large molecular reactions. Johnson and Stein[7] studied the influence of pore structure on catalytic performance and suggested that the ordered macro-pore was favorable for large molecular reactions. Tan et al.[8] reported that macro-meso-micro-porous MY/kaolin composite catalysts exhibited excellent activity in heavy crude oil cracking. Somma et al.[9] prepared niobia-silica xeogel, aerogel and MCM type materials used for epoxidation of cyclohexene with hydrogen peroxide, and found that meso-macro-porous aerogel was a stable and recyclable catalyst.

There are only several reports about macro-porous materials used as catalysts or catalyst supports for small molecule reactions. Liorca et al.[10] reported that macro-porous silicon supported Co_3O_4-ZnO exhibited high efficiency for producing hydrogen from ethanol steam reforming. Guan et al.[11] discovered that Pt-Rh supported on Al_2O_3 inverse opals showed much better catalytic performance than that of Pt-Rh supported on wash-coated Al_2O_3 layers in microchannel reactor. In our previous work, it was found that macro-porous $K-Pt/Al_2O_3$ catalysts showed very good catalytic performance for preferential oxidation of CO in hy-

Foundation item: Project supported by the Ministry of Sciences and Technology of China (863 Programs) (2006AA05Z115, 2007AA05Z104)

Corresponding author: LIU Yuan (**E-mail:** yuanliu@tju.edu.cn; **Tel.:** +86-22-87401675)

DOI: 10.1016/S1002-0721(08)60264-1

drogen-rich gases[12]. It has been proposed in these reports that the good or better catalytic performance is owing to macroporous structure favoring mass transfer.

In this work, 3DOM Pt/TiO_2 and ceria-modified 3DOM Pt/TiO_2 catalysts were prepared and applied to WGS reaction. It was shown that 3DOM catalysts exhibited very good catalytic performance for WGS reaction.

1 Experimental

1.1 Catalyst preparation

Preparation of template: monodispersed polystyrene (PS) beads were prepared with surfactant-free emulsion polymerization of styrene, as reported in literature[13]. 120 ml of the resultant PS beads were poured into a polypropylene tube and centrifuged at a rate of 3000 r/min for 2 h. The sediment was dried at 70 °C for 24 h first. In order to create necks between the adjacent beads, it was then dried at 100 °C for 10 min.

Preparation of 3DOM TiO_2: titanium precursor solutions were prepared by mixing 20 ml of $Ti(OBu)_4$ and 30 ml ethanol under stirring, and 3.2 g H_2O was dropped slowly into the mixed solutions. Then, 1.3 ml of HNO_3 was added into the titanium solutions to form sols, and held at room temperature for 2 d. PS templates were soaked in the titanium sols for 5 min, and then the excess of titanium sol were removed by vacuum filtration. The infiltered templates were dried at 70 °C for 2 h. The infiltration-drying procedure was repeated several times. The resultant composites were calcined in a tube furnace under air flowing at 300 °C for 4 h at a heating rate of 1 °C/min, followed by calcination at 550 °C for 4 h at a heating rate of 2 °C/min.

Preparation of ceria-modified 3DOM TiO_2: ceria was loaded on 3DOM TiO_2 with impregnation method. 3DOM TiO_2 was soaked in $Ce(NO_3)_3$ solutions for 20 h, then it was dried at 80 °C for 8 h. The composites were calcined in a furnace at 500 °C for 3 h at a heating rate of 10 °C/min.

Preparation of 3DOM Pt/TiO_2 and 3DOM Pt/CeO_2-TiO_2: platinum was loaded on 3DOM TiO_2 and 3DOM CeO_2-TiO_2 with impregnation method using H_2PtCl_6 solution as the precursor. The impregnated samples were dried at 70 °C for 12 h and subsequently calcined at 500 °C for 3 h. The mass content of metal platinum in the calcined catalysts is 0.68% for all of the samples.

1.2 Characterization

Macro-porous structure of the samples was characterized by a JSM-6330F scanning electron microscope (SEM). HRTEM images were obtained on a Tecnai G2 F20 electron microscope. The Pt metal content was measured on an inductively coupled plasma atom emission spectroscopy ICP-9000 (N+M). BET surface areas were analyzed by utilizing Micromeritics Tri-Star 3000 sorption analyzer. X-ray diffraction (XRD) patterns of the samples were recorded on a Philip X'pert Pro diffractometer. Cobalt Kα radiation (λ= 0.178901 nm) was used with a power setting of 40 kV and 40 mA.

Temperature-programmed reduction (TPR) of the catalysts was conducted in a fixed-bed continuous flow reactor system with reduction mixture of 5% H_2/Ar at a flow rate of 30 ml/min and at a heating rate of 10 °C/min.

1.3 Catalytic activity measurement

WGS reaction was performed at ambient pressure with a fixed bed flow reactor. Prior to each reaction tests, 50 mg of catalysts was reduced with a flow of 20% H_2/N_2 mixture at 400 °C for 1 h. Then, a gas mixture was introduced into the reactor at 200 °C at a flow rate of 100 ml/min. One feed gas stream consisted of 3% CO and 10% H_2O balanced with N_2. The other feed gas stream simulating reforming gases consisted of 2.5%CO, 3.1%CO_2, 46.1%H_2, 22.5%N_2, and 25.8%H_2O. Product gas streams were analyzed on-line with a gas chromatograph.

2 Results and discussion

2.1 TG-DTA

Fig.1 shows the TG and DTA diagrams of 3DOM TiO_2 before calcination. There is a slow mass loss from room temperature to about 350 °C, due to the evaporation of solvent. The sharp mass loss from 350 to 400 °C is owing to the decomposition and combustion of the PS template, which is an exothermic process. The phase transformation of TiO_2 from anatase to rutile occurs at about 450 °C, which is an exothermic process. So the calcination temperature is set at 550 °C.

2.2 SEM

As shown in Fig.2(a), PS beads are arranged effectively

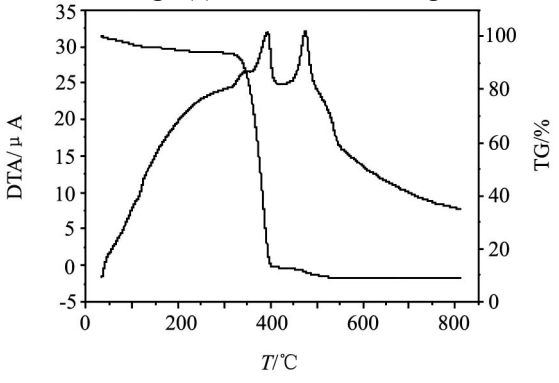

Fig.1 TG and DTA diagrams of 3DOM TiO_2

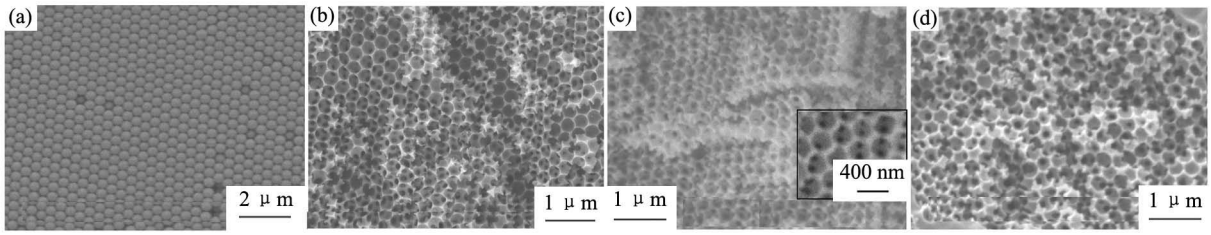

Fig.2 SEM images of PS template (a), 3DOM TiO_2 (b), 3DOM Pt/TiO_2 (c), and 3DOM Pt/10%CeO_2-TiO_2 (d)

into close-packed three-dimensional colloidal crystals. It can be seen that one colloidal particle is connected with surrounding particles through bridges. These bridges could be formed with thermal treatment of the prepared opals due to the expansion of the polymer spheres, which are in close contact with each other.

It is clearly observed from Figs.2(b) and (c) that 3DOM TiO_2 and 3DOM Pt/TiO_2 exhibit a highly ordered and interconnected honeycomb pore structure, which replicate the structure of three-dimensional close-packed PS opals shown in Fig.2(a). The pore sizes of the inverse opals are smaller than that of the original PS sphere template, suggesting that shrinkage occurred during the calcination. Although the shrinkage may lead to some disorder of the three-dimensional ordered macro-pores, the long-range order of the inverse opals remains, as can be seen from Figs.2(b) and (c). The small windows between opal pores are resulted from the contact bridges between the neighboring PS spheres, as can be seen from the inserted image of Fig.2(c), which facilitate reactants diffusing. As shown in Fig.2(d), the long-range order of macro-pores is also observed from the image of Pt/10%CeO_2-TiO_2 inverse opals. Macroporous structure of TiO_2 has been little affected either by loading platinum or by adding CeO_2.

2.3 XRD

XRD patterns of 3DOM Pt/TiO_2 and 3DOM Pt/CeO_2-TiO_2 with different CeO_2 loadings is shown in Fig.3. Anatase and rutile phases of TiO_2 appear in 3DOM Pt/TiO_2 calcined at 550 °C. As shown in Figs.3(2), (3) and (4), the characteristic peaks corresponding to (111) and (200) of CeO_2 are detected for ceria modified samples, and the more CeO_2 loadings, the stronger the ceria diffraction peaks. No peaks corresponding to Pt and PtO_x are detected with XRD.

2.4 High-resolution transmission electron microscopy

Fig.4 shows some typical HRTEM pictures of 3DOM Pt/TiO_2 and 3DOM Pt/CeO_2-TiO_2 with different CeO_2 loadings. The small black dots are PtO_x particles. For all of the samples, the platinum species are uniformly and highly dispersed on the macro-porous supports. The size of platinum particles is about 1 nm, and the size and dispersion of Pt particles are not affected by modification of CeO_2.

TiO_2 and CeO_2 crystals can be distinguished by their lattice stripes, as shown in Fig.4(d). Fig.4(d) is an amplified picture of part of Fig.4(c). It is seen that some Pt particles are loaded on the interface of TiO_2 and CeO_2 crystals, some on ceria crystals (in interaction with titanium oxide) and some

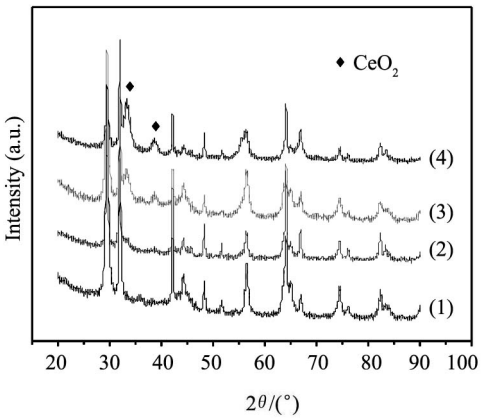

Fig.3 XRD patterns of (1) 3DOM Pt/TiO_2, (2)3DOM Pt/5%CeO_2-TiO_2, (3) 3DOM Pt/10%CeO_2-TiO_2, (4) 3DOM Pt/20%CeO_2-TiO_2

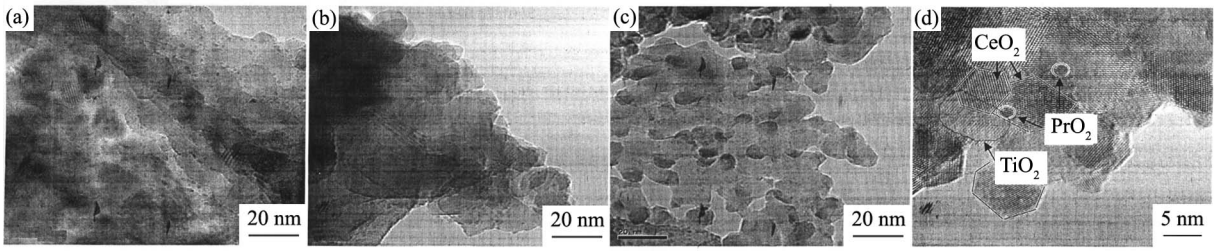

Fig.4 HRTEM images of 3DOM Pt/TiO_2 and 3DOM Pt/CeO_2-TiO_2
(a) 3DOM Pt/TiO_2; (b) 3DOM Pt/5%Ce-Ti; (c) 3DOM Pt/20%Ce-Ti; (d) 3DOM Pt/20%Ce-Ti

on titanium oxide crystals (in interaction with ceria). The interaction formation between ceria and titanium oxide can be verified by the following TPR results.

As ceria loading is low, such as 5wt.%, ceria particles are harder to be seen from HRTEM. However, from XRD, it is deduced that the ceria should be highly dispersed, because the diffraction peaks of ceria are much weak and broad. As ceria loading is higher, such as 20%, ceria particles are uniformly dispersed on TiO_2, as can be seen from Fig.4(c), in which the darker particles with size of about 7 nm are ceria particles (distinguished from lattice stripes with HRTEM).

2.5 TPR

Fig.5 shows the TPR profiles of the 3DOM Pt/TiO_2 and 3DOM Pt/CeO_2-TiO_2 with different CeO_2 loadings. The lower temperature γ peak, centered at about 70 °C, is attributed to the reduction of PtO_x to metal Pt and Ti^{4+} ions on the interface between platinum and titanium oxide particles to Ti^{3+}[14,15]. It is seen that H_2 consumption increases when 3DOM Pt/TiO_2 is modified with CeO_2, indicating that adding CeO_2 facilitates this reduction process. Peak λ, the reduction of PtO_x and ceria on the interface of platinum and ceria particles in 3DOM Pt/CeO_2 (shown in Fig.5(5)), is shifted to higher temperature compared with γ peak, which indicates that PtO_x and ceria on the interface in 3DOM Pt/CeO_2 is harder to be reduced than that of 3DOM Pt/TiO_2. Peak λ appears in Fig.5(4), indicating the existence of interaction of PtO_x and CeO_2 in 3DOM Pt/CeO_2-TiO_2.

Peak α_1 and peak β_1 appear at the temperature range of 200–500 °C, ascribed to the reduction of surface oxygen of support[16,17]. It is known that precious metal facilitates the reduction of support[18]. Peak β_1, the surface reduction of TiO_2, is shifted to higher temperature due to the interaction of TiO_2 and CeO_2. Peak α_1, the surface reduction of CeO_2, appears when ceria content is 20%, and it reveals that some

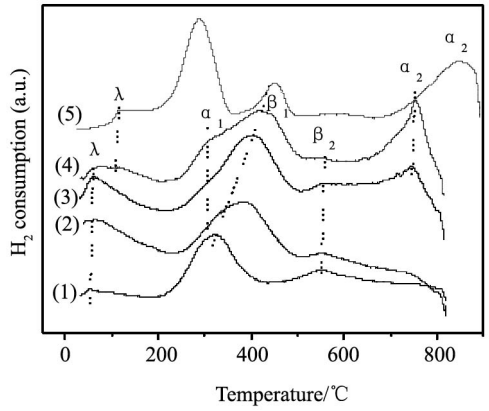

Fig.5 TPR profiles of 3DOM Pt/TiO_2 (1), 3DOM $Pt/5\%CeO_2$-TiO_2 (2), 3DOM $Pt/10\%CeO_2$-TiO_2 (3), 3DOM $Pt/20\%CeO_2$-TiO_2 (4), and 3DOM Pt/CeO_2 (5)

CeO_2 interacts with PtO_x species in 3DOM Pt/CeO_2-TiO_2.

Peak β_2 is assigned to the reduction of bulk TiO_2[19], and adding ceria leads to the shift of this peak position to a little higher temperature. Peak α_2 corresponds to the reduction of bulk CeO_2. By comparing α_2 peak in Figs.5 (3), (4) and (5), it is seen that bulk ceria in Pt/CeO_2-TiO_2 is easier to be reduced than that in Pt/CeO_2.

It is concluded from above that interaction between ceria and TiO_2 is formed. In 3DOM Pt/CeO_2-TiO_2 catalysts, platinum is mainly supported on the surface of TiO_2 and CeO_2, and as ceria content is high, such as 20wt.%, part of Pt/CeO_2 seems to exist. The reductions of PtO_x to metal Pt and Ti^{4+} ions on the interface between platinum and titanium oxide particles to Ti^{3+} are facilitated by modification with CeO_2.

2.6 Catalytic performance test

In order to explore the effect of macro-porous structure on the catalytic performance, 3DOM Pt/TiO_2 was pressed and the catalytic performance for the WGS reaction was tested. It is shown that CO conversion over the pressed catalyst is nearly the same as that over unpressed 3DOM Pt/TiO_2 at reaction temperature of 180 °C. With the increase of reaction temperature, CO conversion over the pressed catalyst is enhanced, but the CO conversion over unpressed 3DOM Pt/TiO_2 is obviously higher. The pressed catalyst shows 51% CO conversion at 360 °C, while 80% CO conversion is achieved over the corresponding catalyst unpressed. Apart from the macro-porous structure, the properties of the two catalysts are the same, thus the different catalytic performance should be caused by the macro-porous structure. The macro-porous structure facilitates reactants diffusing; hence, it is proposed that the better catalytic performance of 3DOM Pt/TiO_2 is owing to the macro-porous structure favoring mass transfer.

Andreeva et al.[19] and Flytzani-Stephanopoulos et al.[20] studied WGS reaction over Au–ceria catalysts, and proposed that nano-size gold particles on the surface in close contact with ceria played a decisive role for its high activity and stability[20]. As for Pt/TiO_2 and Pt/CeO_2 catalysts, similar surface reaction scheme has been put forward, that is, WGS reaction over Pt/TiO_2 or CeO_2 proceeds synergistically on nano-platinum particles and support in close contact with platinum[21–23]. It is assumed that the interface between precious metal and support plays a decisive role for 3DOM Pt/CeO_2-TiO_2. As shown in Fig.6, 3DOM $Pt/10\%CeO_2$-TiO_2 is more active than both 3DOM Pt/TiO_2 and 3DOM Pt/CeO_2. TPR results indicate that adding ceria promotes the reduction of PtO_x and the support on the interface between platinum and support oxides, thus the catalytic activity is

improved by ceria modification. HRTEM and XRD results show that ceria particles are uniformly dispersed on titanium oxide surface, which favors the formation of interaction between ceria and titanium oxide. TPR results obviously suggest the formation of interaction between CeO_2 and TiO_2. Hence, it is pointed out that the added ceria is in interaction with TiO_2, the interaction leads to easier reduction of PtO_x and the interface, the latter results in the improved activity for WGS.

For hydrogen production from hydrocarbons, WGS reaction generally follows steam reforming. The reformed gas mixtures contain not only CO and water, but also CO_2 and H_2. So 3DOM Pt/CeO_2-TiO_2 catalysts were tested for water-gas shift reaction in simulated reformate gas mixture, the results are shown in Fig.7. It is shown that 3DOM Pt/CeO_2-TiO_2 catalysts exhibit very good catalytic performance in the reformed gas mixture at high space velocity of 120,000 ml/(g·h), indicating that 3DOM Pt/CeO_2-TiO_2 is a promising WGS catalyst. With the increase of ceria content, the CO conversion increases (Fig.7). The reason may be that the titanium modified ceria supported platinum catalyst is more active, as ceria content is 20wt.%, therefore, part of the catalyst exhibits the property of titanium modified Pt/CeO_2.

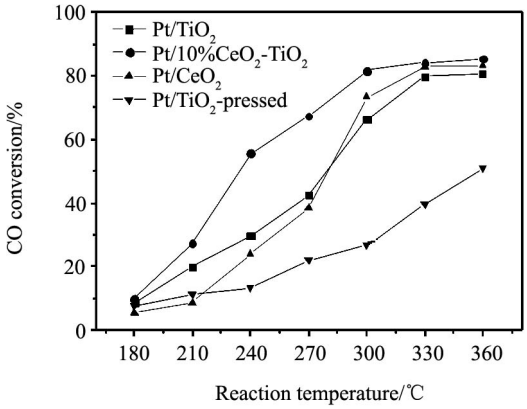

Fig.6 Effect of CeO_2 on the activity for the WGS reaction (0.68%Pt; feed gas: 3%CO, 10%H_2O, 87%N_2; total flow rate: 100 ml/min; GHSV:120,000 ml/(g·h))

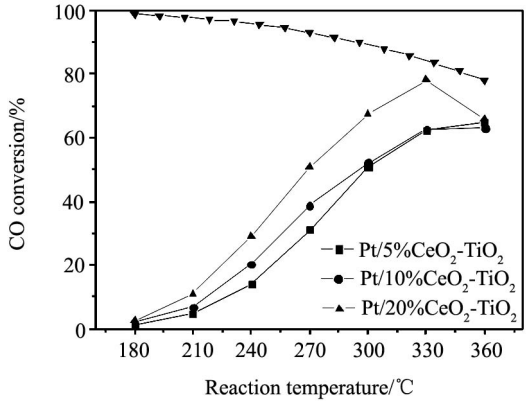

Fig.7 Effects of CeO_2 loadings on the activity of 3DOM Pt/CeO_2-TiO_2 for the WGS reaction (0.68%Pt; feed gas: 2.5%CO, 3.1%CO_2, 46.1%H_2, 22.5%N_2, 25.8%H_2O; total flow rate: 100 ml/min; GHSV: 120000 ml/(g·h))

3 Conclusion

Novel catalysts consisting of Pt crystallites deposited over 3DOM TiO_2 and cerium-modified 3DOM TiO_2 substrate were prepared with template and impregnation methods. 3DOM catalysts exhibited much better catalytic performance than that without macro-porous structure for WGS reaction, which was owing to macro-porous structure favoring mass transfer.

Ceria modified 3DOM Pt/TiO_2 showed better catalytic performance than 3DOM Pt/TiO_2. Addition of ceria promoted the reduction of PtO_x and the support on the interface between platinum and support oxides, thus the catalytic activity was improved by ceria modification.

Owing to the special porous structure of three dimensionally ordered macro-porous materials and the modification role of ceria, the 3DOM Pt/CeO_2-TiO_2 materials should be a potentially attractive kind of catalyst for WGS reaction.

References:

[1] Jiang Lilong, Ye Binghuo, Weik Emei. Effects of CeO_2 on structured and properties of Ni-Mn-K/bauxite catalysts for water-gas shift reaction. *Journal of Rare Earths*, 2008, **26**: 352.

[2] Mendelovici L, Steinberg M. Methanation and water-gas shift reactions over Pt/CeO_2. *Catal.*, 1985, **96**: 285.

[3] Azzam K G, Babich I V, Seshan K, Lefferts L. Single stage water gas shfit conversion over Pt/TiO_2-Problem of catalyst deactivation. *Appl. Catal. A: Gen.*, 2008, **338**: 66.

[4] Jacobs G, Ricote S, Patterson P M, Graham U M, Dozier A, Khalid S, Rhodus E, Davis B H. Low temperature water-gas shift: Examining the efficiency of Au as a promoter for ceria-based catalysts prepared by CVD of a Au precursor. *Appl. Catal. A: Gen.*, 2005, **292**: 229.

[5] Bunluesin T, Gorte R J, Graham G W. Studies of the water-gas-shift reaction on ceria-supported Pt, Pd, and Rh: implications for oxygen-storage properties. *Appl. Catal. B: Environ.*, 1998, **15**: 107.

[6] Schroden R C, Al-Daous M, Sokolov S, Melde B J, Lytle J C, Stein A, Carbojo M C, Ferna´ndez J T, Rodrı´guez E E. Hybrid macroporous materials for heavy metal ion adsorption. *Mater. Chem.*, 2002, **2**: 3261.

[7] Johnson B J S, Stein A. Surface modification of mesoporous, macroporous, and amorphous silica with catalytically active polyoxometalate clusters. *Inorg. Chem.*, 2001, **40**: 801.

[8] Tan Q, Bao X, Song T, Fan Y, Shi G, Shen B, Liu C, Gao X. Synthesis, characterization, and catalytic properties of hydrothermally stable macro-meso-micro-porous composite materi-

als synthesized via in situ assembly of preformed zeolite Y nanoclusters on kaolin. *Catal.*, 2007, **251**: 69.

[9] Somma F, Strukul G. Niobium containing micro-, meso- and macroporous silica materials as catalysts for the epoxidation of olefins with hydrogen peroxide. *Catal. Lett.*, 2006, **107**: 73.

[10] Llorca J, Casanovas A,Trifonov T, Rodríguez A, Alcubilla R. First use of macroporous silicon loaded with catalyst film for a chemical reaction: A microreformer for producing hydrogen from ethanol steam reforming. *Catal.*, 2008, **255**: 228.

[11] Guan G, Zapf R, Kolb G, Hessel V. Preferential CO oxidation over catalysts with well-defined inverse opal structure in microchannels. *Int. J. Hydrogen Energy*, 2008, **33**: 797.

[12] Zhang Y, Zhao C Y, Liang H, Liu Y. Macroporous monolithic Pt/γ-Al_2O_3 and K-Pt/γ-Al_2O_3 catalysts used for preferential oxidation of CO. *Catal. Lett.*, 2009, **127**: 339.

[13] Dionigi C, Nozar P, Domenico D D, Calestani G. A simple geometrical model for emulsifier free polymer colloid formation. *Col. Inter Sci.*, 2004, **275**: 445.

[14] Zhang C, He H, Tanaka K. Catalytic performance and mechanism of a Pt/TiO_2 catalyst for the oxidation of formaldehyde at room temperature. *Appl. Catal. B: Environ.*, 2006, **165**: 37.

[15] Panagiotopoulou P, Christodoulakis A, Kondarides D I, Boghosian S. Particle size effects on the reducibility of titanium dioxide and its relation to the water-gas shift activity of Pt/TiO_2 catalysts. *Catal*., 2006, **240**: 114.

[16] Epling W S, Cheekatamarla P K, Lane A M. Reaction and surface characterization studies of titania-supported Co, Pt and Co/Pt catalysts for the selective oxidation of CO in H_2-containing streams. *Chem. Eng. J.*, 2003, **93**: 61.

[17] Pe´rez-Herna´ndez R, Go´mez-Corte´s A, Arenas-Alatorre J, Rojas S, Mariscal R, Fierro J L G, Dı´az G. SCR of NO by CH_4 on Pt/ZrO_2-TiO_2 sol-gel catalysts. *Catal. Today*, 2005, **107–108**: 149.

[18] Peng J, Wang S. Performance and characterization of supported metal catalysts for complete oxidation of formaldehyde at low temperatures. *Appl. Catal. B: Environ.*, 2007, **73**: 282.

[19] de Resende N S, Eon J G, Schmal M. Pt-TiO_2-γ-Al_2O_3 catalyst I. dispersion of platinum on alumina-grafted titanium oxide. *Catal.*, 1999, **183**: 6.

[20] Tabakova T, Boccuzzi F, Manzoli M, Sobczak J W, Idakiev V, Andreeva D. Effect of synthesis procedure on the low-temperature WGS activity of Au/ceria catalysts. *Appl. Catal. B: Environ.*, 2004, **49**: 73.

[21] Fu Q, Saltsburg H, Flytzani-Stephanopoulos M. Active nonmetallic Au and Pt species on ceria-based water-gas shift catalysts. *Science*, 2003, **301**: 935.

[22] Fu Q, Deng W, Saltsburg H, Flytzani-Stephanopoulos M. Activity and stability of low-content gold-cerium oxide catalysts for the water-gas shift reaction. *Appl. Catal. B: Environ.*, 2005, **56**: 57.

[23] Goguet A, Meunier F, Breen J P, Burch R, Petch M I, Ghenciu A F. Study of the origin of the deactivation of a Pt/CeO_2 catalyst during reverse water gas shift (RWGS) reaction. *Catal.*, 2004, **226**: 382.